OXFORD

Original Article

Lineage diversification of the Sky Island treefrog *Scinax curicica* (Anura, Hylidae) in the Espinhaço Mountain Range

Diego J. Santana[1,*], Eric Ragalzi[1], Ricardo Koroiva[2,3], Sarah Mângia[1], Karoline Ceron[4], Felipe S.F. Leite[5], Donald B. Shepard[6]

[1]Instituto de Biociências, Universidade Federal de Mato Grosso do Sul, Av. Costa e Silva, s/n, 79070-900, Campo Grande, Mato Grosso do Sul, Brazil
[2]Departamento de Sistemática e Ecologia, Universidade Federal da Paraíba, Cidade Universitária, 58051-090, João Pessoa, Paraíba, Brazil
[3]Instituto de Ciências Biológicas, Universidade Federal do Pará, Rua Augusto Corrêa, 66075-110, Belém, Pará, Brazil
[4]Laboratório de Estrutura e Dinâmica da Diversidade, Instituto de Biologia, Universidade Estadual de Campinas, Rua Monteiro Lobato, 255, 13083-862, Campinas, Brazil
[5]Instituto de Ciências Biológicas e da Saúde, Universidade Federal de Viçosa, Campus Florestal, Rodovia LMG 818, km 6, 35690-000, Florestal, Minas Gerais, Brazil
[6]School of Biological Sciences, Louisiana Tech University, Carson-Taylor Hall, 1 Adams Blvd, 71270, Ruston, LA, United States

*Corresponding author. Instituto de Biociências, Universidade Federal de Mato Grosso do Sul, Campo Grande, Mato Grosso do Sul, Brazil. E-mail: jose.santana@ufms.br

ABSTRACT

Sky Islands present unique landscapes for organismal evolution because they comprise high mountain peaks separated by low valleys with vastly different environmental conditions. The Espinhaço Mountain Range in eastern Brazil is formed of groups of Sky Islands in the states of Minas Gerais and Bahia. Several phylogeographic studies have discovered strong genetic structure among populations of organisms occupying the *campo rupestre* (rupestrian fields) in the mountains of the Espinhaço. In this study, we aimed to test the hypothesis of spatio-temporal structuring of populations of *Scinax curicica* in the *campo rupestre* of the Espinhaço. We recovered three lineages of *S. curicica*: one lineage occurs in the north portion of the Espinhaço (North Lineage) in an area called Chapada Diamantina, and other two occur in the south portion of the Espinhaço (South 1 and South 2 Lineages) in Minas Gerais. All three lineages showed stable population sizes through time, probably due to the climatic stability of mountaintop areas, which was supported by ecological niche modelling.

Keywords: campos rupestres; phylogeography; speciation; treefrog; climatic oscillations

INTRODUCTION

Montane areas in tropical regions are often called 'cradles of biodiversity' and 'species pumps' because of their high species richness (García-Rodríguez *et al.* 2021). The ecological and evolutionary processes generating and maintaining high biodiversity in montane regions is an active area of research (Graham *et al.* 2014, Rahbek *et al.* 2019). Some mountain ranges referred to as Sky Islands present unique landscapes for organismal evolution because they comprise high mountain peaks separated by low valleys with vastly different environmental conditions (e.g. temperature, humidity, vegetation). These valleys act as barriers to the dispersal between populations of organisms adapted to environmental conditions at higher elevations, leading to isolation and divergence of populations on different mountains (McCormack *et al.* 2011, Sekar and Karanth 2013). Within

high-altitude areas, usually above 1000 m a.s.l., elevational variation in environmental conditions can also result in barriers to dispersal and gene flow in some species or dispersal corridors for others, depending on their ecology (Haffer and Prance 2002, Salerno *et al.* 2012). Furthermore, these are dynamic systems in which environmental changes may result in alternating periods of isolation and connection of populations. Such histories are often manifest in the distributions and population genetic structure of organisms, and even with the diversification of species, as has been shown in species of lizards (Sinervo *et al.* 2010), mammals (Beever *et al.* 2011), and amphibians (Shepard and Burbrink 2008, 2009, Salerno *et al.* 2012).

The Espinhaço Mountain Range (hereafter Espinhaço) in eastern Brazil is formed of groups of smaller ranges (Sky Islands) in the states of Minas Gerais and Bahia, extending approximately

1200 km from north to south, with altitudes varying from 800 to 2000 m a.s.l. The Espinhaço form a border between the Atlantic Forest to the east and the open, savanna landscapes of the Cerrado and Caatinga bioregions to the north and west (Guedes *et al.* 2020). The Espinhaço is divided into two main portions (from north to south): the north portion of the Espinhaço in Bahia State, known as Chapada Diamantina and the south portion, which extends from south-western border of Chapada Diamantina to the Quadrilátero Ferrífero region representing its southernmost limit, in Minas Gerais State.

Along the length of the Espinhaço, different altitudes rise to a variety of climatic conditions and habitats, with the *campo rupestre* (rupestrian fields) being the predominant formation at altitudes above 1000 m a.s.l. (Schaefer *et al.* 2016, Miola *et al.* 2021). The *campo rupestre* is characterized as a high-altitude mosaic of grassy-shrubby vegetation, interspersed with rocky outcrops, and encompassing grasslands with patches of transitional vegetation from Caatinga, Cerrado, and Atlantic Forest (Silveira *et al.* 2016). In terms of its ecological significance, *campo rupestre* has been identified as microrefugia during the interglacial periods of the Pleistocene, providing shelter for species adapted to cold and drought in tropical regions (Collevatti *et al.* 2012, Bonatelli *et al.* 2021). These rocky outcrops acted as refuges for species during climatic fluctuations, helping to maintain local biodiversity. Furthermore, research suggests that the cyclic expansion and contraction of species ranges during Quaternary climate changes have played a significant role in shaping the current levels of population genetic structure for *campo rupestre* species (Barres *et al.* 2019, Oliveira *et al.* 2021). These historical range dynamics have contributed to the genetic differentiation and isolation of populations, leading to unique genetic signatures within *campo rupestre* species.

Several recent phylogeographic studies have been published on endemic anuran species in the *campo rupestre* (Carvalho *et al.* 2020, Oliveira *et al.* 2021, Oswald *et al.* 2022); however, these focused on species restricted to the southern or northern portion of the Espinhaço. Nonetheless, these studies have demonstrated that, even at a smaller spatial scale, the mountains comprising the southern Espinhaço act as Sky Islands, generating strong genetic structure among populations of organisms occupying these rocky meadows. The leaf frog *Pithecopus megacephalus* was found to comprise three phylogeographic lineages, with one exclusively from a separate area in north Minas Gerais (Magalhães *et al.* 2017). The treefrog *Bokermannohyla saxicola*, another species endemic to the southern portion of the Espinhaço, was recently found to consist of four lineages that diverged from the Pliocene to Early Pleistocene (Oswald *et al.* 2022). A species from the same genus, *Bokermannohyla alvarengai*, which also occurs in the southern Espinhaço, was shown to comprise two geographically distinct lineages (Oliveira *et al.* 2021). Despite the number of lineages differing among these taxa, the genetic breaks appear concordant geographically, with the mountains in northern Minas Gerais separated from the others. One of the few studies with frogs from the northern portion of the Espinhaço in Bahia (Chapada Diamantina), was conducted with *Bokermannohyla oxente*, which is structured in two lineages even within its small distribution (Oliveira *et al.* 2021).

Among amphibians, treefrogs of the genus *Scinax* Wagler, 1830 form the second most diverse genus in Hylidae, and are represented by a wide range of species occupying different environmental conditions in the Neotropics (Faivovich *et al.* 2005). For some species of this genus, occurrence in the *campo rupestre* of the Espinhaço has been an important factor in speciation. Examples include the narrow endemic *Scinax cabralensis* found exclusively in Serra do Cabral, Minas Gerais, on the western slopes of the southern portion of the Espinhaço (Drummond *et al.* 2007), *Scinax machadoi*, which is endemic to the southern portion of the range (Leite *et al.* 2008), and *Scinax montivagus*, which is found only in Chapada Diamantina, Bahia, in the north portion of the Espinhaço (Juncá *et al.* 2015). In the Espinhaço, *Scinax curicica* occupies *campo rupestre* areas (Pugliese *et al.* 2004) with a discontinuous distribution along the whole Espinhaço, exclusively at altitudes above 850 m a.s.l. (Leite *et al.* 2006, 2008). The species reproduces mainly in permanent lentic environments, but also in small slow-flowing streams (Eterovick 2003, Pugliese *et al.* 2004).

Our study focuses on the spatio-temporal structuring of *S. curicica* populations in the *campo rupestre* of the Espinhaço. We propose that Pleistocene climate changes and the unique landscape of altitude islands played a key role in the species' diversification. These climate fluctuations prompted habitat shifts and speciation in various organisms. The EMR, with isolated high-altitude areas, created a fragmented landscape enabling geographic isolation and limited gene flow among *S. curicica* populations. These geographic barriers, combined with Pleistocene climatic variability, likely led to distinct genetic lineages. Accordingly, we predict genetic differentiation and unique adaptations in *S. curicica* populations across the *campo rupestre* of the EMR, reflecting specific local environments. We used phylogenetic analysis of mitochondrial and nuclear DNA, divergence dating, historical demography analysis, and ecological niche modelling (ENM) to examine the population history of this species. Specifically, we evaluated the evolutionary history and the effects of Quaternary climate change on the population demography of *S. curicica*, predicting that mountaintops act as Sky Islands, driving the diversification of genetic lineages within this endemic Espinhaço treefrog.

MATERIAL AND METHODS

Taxon sampling

DNA was sampled from 51 specimens from 13 sites along the Espinhaço (Fig. 1; Supporting Information, Table S1). Tissue was removed from either the thigh muscle or the liver. All samples were preserved in absolute (100%) alcohol and stored in a freezer at -20 °C until the time of DNA extraction. Voucher specimens are housed in the Amphibian Collection of the Universidade Federal de Minas Gerais (UFMG-AMP) (Supporting Information, Table S1). We conducted this study under Sistema de Autorização e Informação em Biodiversidade (SISBIO) license number ICMBio 21185-1.

DNA extraction, amplification, and sequencing

We extracted genomic DNA using either the CTAB technique or a Qiagen DNeasy Blood and Tissue® Kit (QIAGEN GmbH, Hilden, Germany). We performed PCR using specific primers for amplifying the mitochondrial 16S rRNA gene: 16sAR (CGCCTGTTTATCAAAAACAT) and 16sBR
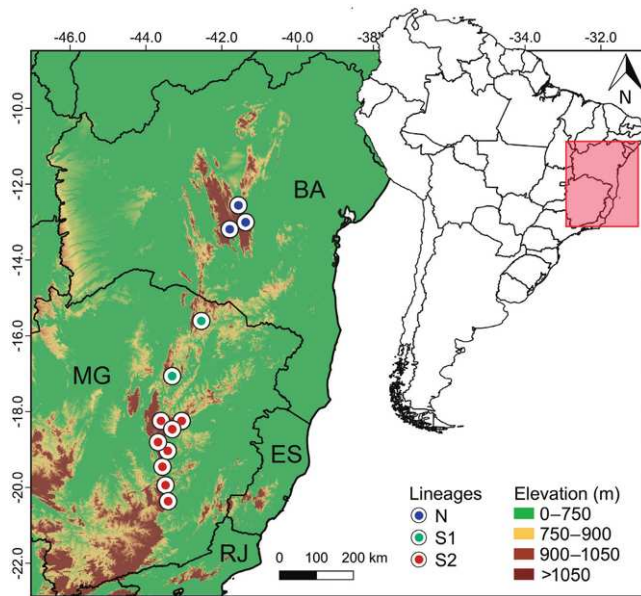
Figure 1. Topographic map showing the known geographic distribution of *S. curicica* in white circles. All genetic samples used in this study are illustrated by coloured circles within white circles coded by lineage. Abbreviations are as follows: MG—Minas Gerais, BA—Bahia, ES—Espírito Santo, RJ—Rio de Janeiro.

(CTCCGGTTTGAACTCAGATCA) (Palumbi *et al.* 1991). We also amplified a portion of the nuclear-encoded *RHOD* (rhodopsin) gene using the following primers: Rhod1A (ACCATGAACGGAACAGAAGGYCC) and Rhod1C (CCAAGGGTAGCGAAGAARCCTTC) (Bossuyt and Milinkovitch 2000). Reactions contained 0.5 U of GoTaq G2 Hotstart DNA polymerase (Promega), 1 × PCR buffer, 0.25 mM of each dNTP, 2 mM of $MgCl_2$, and 0.25 mM of each primer. PCR conditions followed Costa *et al.* (2016) and Mângia *et al.* (2020). We purified PCR products using the Acetate-Ammonium technique (Irwin *et al.* 2003) and we verified the quality of the purified DNA using a NanoDrop® ND-1000 spectrophotometer (Thermo Scientific, USA). Purified PCR products were then sequenced on an ABI 3500 Genetic Analyzer (Applied Biosystems, USA). We aligned sequences with Geneious® R9 9.1.3 (Biomatters Ltd, Auckland, New Zeland).

Mitochondrial phylogeny and molecular dating

We estimated a Bayesian gene tree for the 16S rRNA locus using BEAST 2.6 (Bouckaert *et al.* 2019). The most appropriate substitution model was GTR+I+G, which was determined using jModelTest (Darriba *et al.* 2012). We used a Yule speciation prior, implemented a strict-clock rate of 0.00735 (minimum of 0.0061; maximum of 0.0087) substitutions per site per million years (Gehara *et al.* 2014) with a uniform distribution prior, and ran the analysis for 50 million generations sampling every 5000 generations. We used Tracer 1.7.1 (Rambaut *et al.* 2018) to assess effective sample sizes (ESS) of estimated parameters and stationarity, ensuring that ESSs of all parameters were > 200 (Rambaut *et al.* 2018).

Population analysis assignment and genetic diversity

We performed analysis of population structure in GENELAND 4.0.3 (Guillot *et al.* 2005) as implemented in R 3.1.1 (R Core Team 2015). GENELAND analysis is a spatial genetic analysis tool that applies Bayesian methods to genetic data. It assumes that genetic information shows spatial patterns and aims to identify the number and locations of distinct populations. GENELAND deals with spatial genetic structure and population boundaries within a specific geographic region (Guillot *et al.* 2005). For this analysis, we used 16S rRNA sequences. We determined *K* by the Markov chain Monte Carlo method (MCMC) with six repetitions of *K* from 1 to 5. This range was chosen based on the main clades found in the mtDNA tree. We also performed species delimitation analysis using the generalized mixed Yule coalescence (GMYC) and multi-rate Poisson tree process (mPTP) methods. Both methods aim to identify species boundaries based on patterns observed in molecular phylogenies, given that GMYC employs the Yule process to model speciation and coalescence events (Fujisawa and Barraclough 2013), whereas mPTP determines the transition from a between- to a within-species process, incorporating different levels of intraspecific diversity deriving from differences in either the evolutionary history or sampling of each species (Kapli *et al.* 2017). In addition, mPTP has demonstrated superiority over PTP and other widely-used distance-based approaches, consistently providing more accurate delimitations in accordance with taxonomy (Blair and Bryson 2017, Kapli *et al.* 2017). For both analyses, we used the ultrametric 16S rRNA phylogenetic tree generated in BEAST. The GMYC approach was carried out in R 4.2.3 (R Core Team 2023) using the *splits* (Ezard *et al.* 2010) and *ape* (Paradis *et al.* 2004) packages.

Finally, we built haplotype networks for each of the genes using the median-joining method (Bandelt *et al.* 1999) implemented in Population Analysis with Reticulate Trees (PopART), using the standard configurations (Leigh and Bryant 2015). We calculated the number of haplotypes (*h*), haplotype diversity (*Hd*), and nucleotide diversity (*π*) for each mitochondrial and nuclear locus for each of the lineages identified by the GMYC and mPTP analysis using DnaSP (Rozas *et al.* 2017). We quantified genetic differentiation among and within lineages through Analysis of Molecular Variance (AMOVA) as implemented in PopART (Leigh and Bryant 2015).

Historical demography

We evaluated past changes in effective population size (N_e) of each lineage using the Bayesian Skyline Plot (BSP) method implemented in BEAST 2.6 (Bouckaert *et al.* 2019). For the BSPs, we used an average substitution rate of 0.00735 (with a minimum of 0.0061 and a maximum of 0.0087) substitutions per site per million years (Gehara *et al.* 2014) and the GTR+I+G substitution model. Each BSP analysis was evaluated with a piecewise-linear population function, five groups, 50 million generations, and 10% burn-in. We checked for stationarity by visually inspecting trace plots and ensuring that all values for effective sample sizes (ESS) were above 200 in Tracer 1.7.1 (Rambaut *et al.* 2018). We copied the curve values from Tracer 1.7.1 and built the BSP curve in Microsoft Excel.

Ecological niche modelling

In order to elucidate the effect of Quaternary climate change on the population structure of *S. curicica*, we used an ENM approach to model the species' potential distribution under past climate change scenarios. Current and historical (6 kya, 21 kya,

and 120 kya) climatic data consisted of the 19 standard Bioclim variables (30 arc-seconds resolution) (Fick and Hijmans 2017). This period was selected because it represents the climatic extremes during the past 120 kya and other authors suggest that important climatic changes occurred in the *campo rupestre* during this period (Carvalho *et al.* 2020, Magalhães *et al.* 2021). We analysed a total of 26 occurrence records prior to filtering from the databases of the Mapinguari Laboratory at the Federal University of Mato Grosso do Sul, and the Sagarana Laboratory at the Federal University of Viçosa - Campus Florestal, Brazil. To avoid overprediction and low specificity, we cropped the environmental layers to span from -25° to -10° latitude and -48° to -38° longitude. Locality data were spatially filtered at 2 km² using the R package *spThin* (Aiello-Lammens *et al.* 2015) to eliminate spatial clusters of localities, which resulted in 23 spatially independent occurrence locations for modelling. To avoid bias related to multicollinearity of environmental explanatory variables, we calculated the Variance Inflation Factor (VIF) values for variables. All values that were highly correlated (VIF > 5) were removed through a stepwise procedure, using the *usdm* R package v.1.1-18 (Naimi 2017). Thus, we retained five of the 19 bioclimatic variables that were used throughout this study (Bio1—Annual Mean Temperature, Bio2—Mean Diurnal Range, Bio3—Isothermality, Bio14—Precipitation of Driest Month, Bio18—Precipitation of Warmest Quarter).

We performed species distribution modelling on *S. curicica* using nine different algorithms implemented in the 'biomod2' package (Thuiller *et al.* 2016) in R 4.1 (R Core Team 2021) including the following: three regression methods [GAM: general additive model (Hastie and Tibshirani 1990), GLM: general linear model (McCullagh and Nelder 1989), MARS: multivariate adaptive regression splines (Friedman 1991)]; three machine learning methods [GBM: generalized boosting model (Ridgeway 1999), MAXENT: Maximum Entropy (Phillips *et al.* 2006), RF: random forest (Breiman 2001)], two classification methods [CTA: classification tree analysis (Breiman 1984), FDA: flexible discriminant analysis (Hastie *et al.* 1994)], and one envelope model [SRE: Surface Range Envelop (Booth *et al.* 2014)]. To meet the criteria of having absence (or pseudo-absence) data for most of these models (except SRE), we generated two equal-sized (to the true presence records) sets of random pseudo-absence (PA) points across the model background (500 PA points in each set). The models were calibrated using 70% of randomly selected data. The other 30% of the data were used for intrinsic model evaluation.

Individual model performance was evaluated using two metrics—true skill statistic (TSS) and the area under the curve of receiver operating characteristics (ROC) implemented in the 'biomod2' package. TSS is calculated as 'sensitivity + specificity -1' and ranges from -1 to +1, where +1 indicates perfect agreement, a value of 0 implies agreement expected by chance, and a value of less than 0 indicates agreement lower than expected by chance. Models with high predictive accuracy (TSS > 0.8) were used for the projection of anuran distribution. We constructed ensemble maps based on the median of two runs of all the selected models in which individual accuracy had a TSS value equal to or greater than 0.8. Regions of habitat stability through time were identified by stacking and averaging the current and three projected-palaeoclimate ENMs. Regions highlighted in

these stacked projects were inferred to be regions of climate refugia through time for *S. curicica*.

RESULTS

Mitochondrial phylogeny and molecular dating

The 16S rRNA gene tree topology recovered three main clades in *S. curicica* (Fig. 2). One lineage occurs in the north portion of the Espinhaço (North Lineage), in the Chapada Diamantina region, precisely in the Serra da Almas, Serra da Tromba, and Serra do Sincorá, and the other two lineages occur in the South Espinhaço (South 1 and South 2 Lineages) in Minas Gerais (Fig. 1). South 1 Lineage occurs from the Quadrilátero Ferrífero region, along the Serra do Cipó. South 2 Lineage occurs in the Serra de Itacambira and Serra Nova (Supporting Information, Table S1).

The three main clades, which corresponded to the three lineages, were recovered with strong support of posterior probability (pp ≥ 0.99; Fig. 2). The divergence between the North Lineage and Southern Lineages occurred around 2.51 Mya (95% HPD: 1.73–3.35 Mya), and the separation between the two South lineages dated to about 1.68 Mya (95% HPD [Highest Posterior Density]: 1.11–2.31 Mya; Fig. 2).

### Population analysis assignment and genetic diversity

Using both mtDNA and nuDNA loci, GENELAND detected three populations corresponding to the three mitochondrial lineages (K = 3; Fig. 3; Supporting Information, Fig. S1), and revealed a clear geographical population structure concordant with the different regions of the Espinhaço. The GMYC and mPTP (likelihood ratio: 9.364408; Null-model score: -47.635644) species delimitation methods yielded identical results, recovering the same three evolutionary entities (Fig. 2).

The 16S rRNA haplotype network revealed high haplotype diversity with no shared haplotypes among the three lineages (Fig. 2). Despite high diversity in mtDNA, our haplotype network of the nuclear-encoded *RHOD* gene showed only two haplotypes with no congruence with geographic distributions. In our AMOVA analysis, we found a high index of fixation for the mitochondrial 16S rRNA (Fst = 0.93924, $P < 0.001$), whereas the index of fixation was low for *RHOD* (Fst = 0.41322, $P < 0.001$), indicating most of the variation in *RHOD* occurs among localities rather than among populations.

Historical demography and ecological niche modelling

The North population of *S. curicica* had the most recent coalescent point, approximately 47 kya. On the other hand, both South 1 and South 2 populations had their coalescent points around 300 kya. Despite the different coalescent times, all three populations show stable effective population sizes (N_e) through time (Fig. 4).

The resulting ensemble models based on nine SDM algorithms yielded average values of TSS = 0.97 and ROC = 0.99. The variable Bio1 (annual mean temperature) was the most important variable (63% of explication) to *S. curicica* distribution, followed by precipitation of driest month (Bio14, 36% of explanation) and precipitation of warmest quarter (Bio18, 33% of explication). The potential distribution for *S. curicica* (Fig. 5) generated by ENMs for the present coincides well with
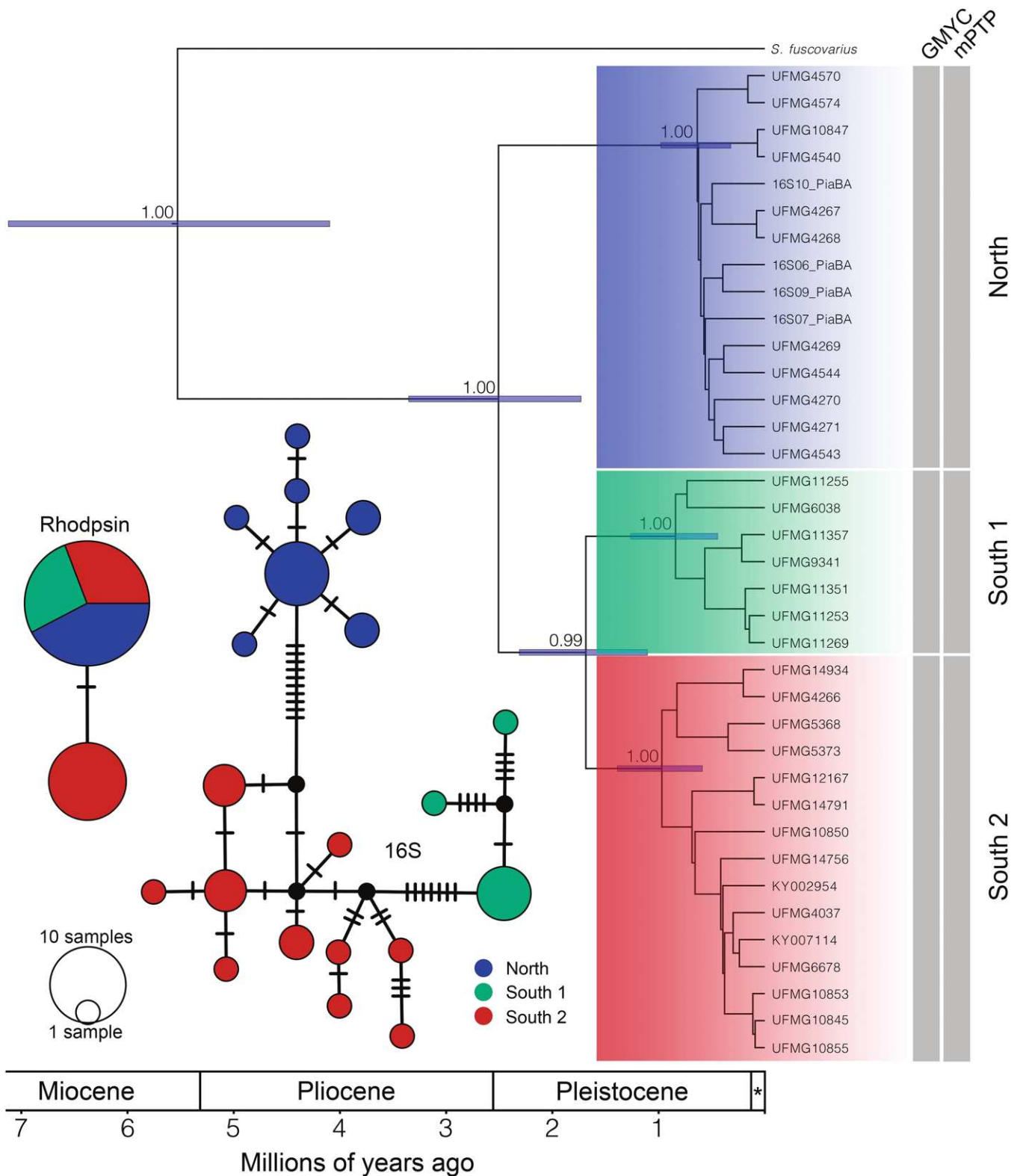
Figure 2. Phylogeny and divergence times of *S. curicica* lineages estimated in BEAST, with results from GMYC and mPTP analysis. Haplotype networks from neighbour-joining analysis for the two genes (16S rRNA and Rhodopsin). Crossed traits indicate additional mutational steps for branches with more than one mutation. Different colours indicate species-level units. The black dots are median vectors (hypothesized sequences).

the species known distribution throughout the Espinhaço, although it also predicts suitable conditions exist in other mountainous areas in south-eastern Brazil, including part of the Serra da Mantiqueira Mountain Range, and other highlands in the Cerrado ecoregion. The predicted distribution for the Holocene (6 kya) climate indicates minor changes for *S. curicica*. However,
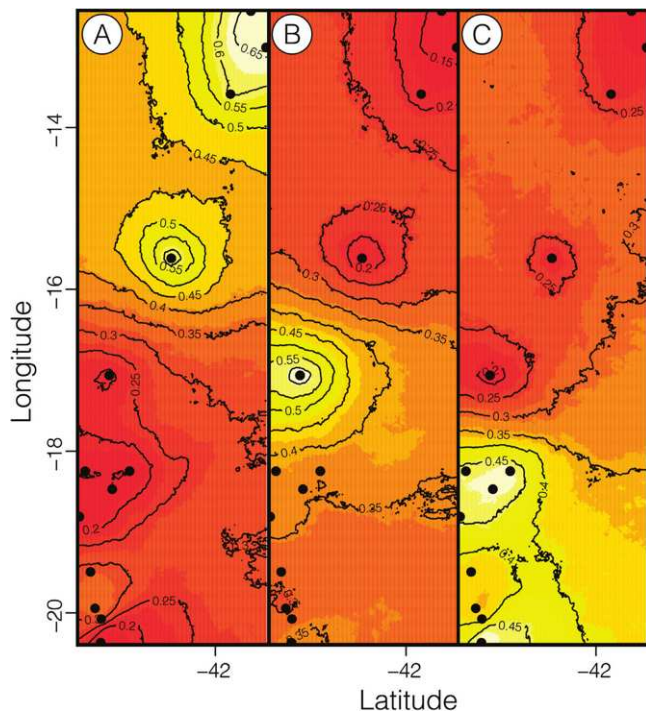
Figure 3. GENELAND analysis of *S. curicica* with posterior probability isoclines, indicating extensions of the genetic populations found (black lines with inclusion probabilities). Light colour zones in maps indicate the groups of localities with greater probabilities of belonging to the same genetic unit. Black dots indicate locations of the 13 analysed localities. (A) North population, (B) South 1 population, and (C) South 2 population.

during the Last Glacial Maximum (21 kya) the potential distribution was immensely expanded throughout surrounding regions. The predicted distribution of *S. curicica* during the Last Interglacial (120 kya) was similar to the current and Holocene periods but slightly more expansive. The stability map generated with all four distribution models suggests suitable regions with a similar distribution to the current known distribution for this species, predicting mainly the highlands of the Espinhaço.

DISCUSSION

We found that *S. curicica* comprises three geographically distinct lineages that originated at the Pliocene–Pleistocene boundary (~2.51 Mya) and in the Early Pleistocene (~1.68 Mya). The three lineages, which were supported by the GENELAND analysis and in both species' delimitation methods, have remained distinct throughout much of the Pleistocene. Our ENMs suggested climatically stable regions very similar to the current species' distribution, which coincides with the Sky Islands of the Espinhaço Range (elevations > 1000 m a.s.l.). Our models indicate potentially suitable habitat for this taxon has not shifted greatly through time, despite the great expansion over 21 kya, which supports a strong relationship with a *campo rupestre* mountaintop habitat for this species. The climatic scenario in Sky Islands is known for promoting diversification in several amphibians throughout the globe (Shepard and Burbrink 2008, 2009, Salerno *et al.* 2012, Pan *et al.* 2019), including in other mountain complexes in southern Brazil (Pie *et al.* 2018) and even for
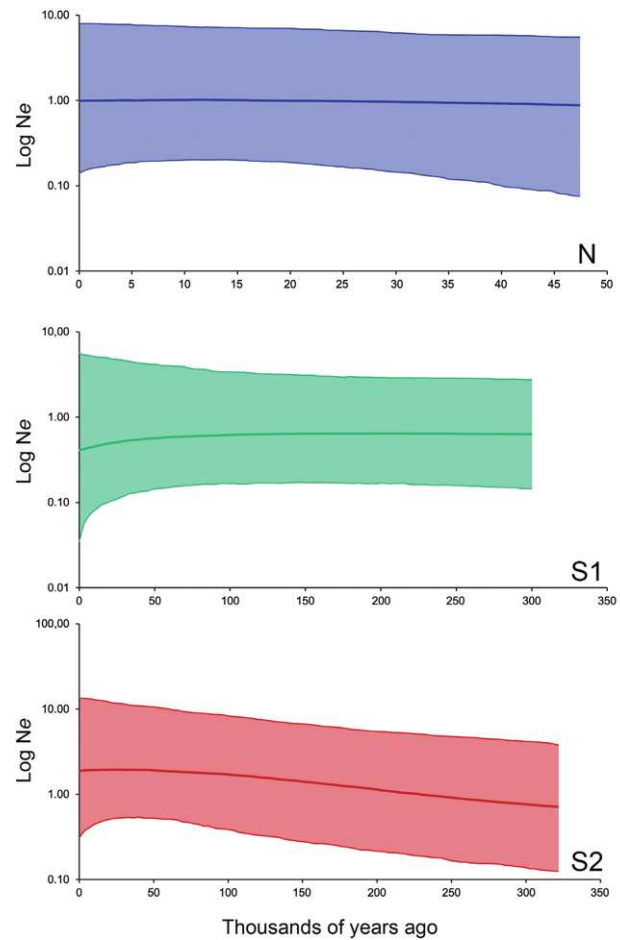
Figure 4. Bayesian skyline plots illustrating effective population sizes (N_e) through time for the three *S. curicica* lineages: North (N), South 1 (S1), and South 2 (S2). The darker inner line represents median population size, and the shaded area represents 95% HPD.

other hylids in the Espinhaço (Carvalho *et al.* 2020, Magalhães *et al.* 2021, Oliveira *et al.* 2021, Oswald *et al.* 2022). Our findings for *S. curicica* corroborate the same climatic scenario for the other hylids from Espinhaço, in which mountaintops acted as refugia during the climatic oscillations of the Pleistocene, promoting allopatric divergence (Nascimento *et al.* 2018, Oliveira *et al.* 2021, Oswald *et al.* 2022). The stable population sizes for the three lineages we recovered also supports the stability of climate and habitat on mountaintops along the Espinhaço.

Consistent with the Espinhaço being Sky Islands, climatic breaks are evident along the range, with a marked break between the northern (Chapada Diamantina) and southern portions, and other discrete breaks in the southern portion (Fig. 5). These breaks coincide with the distributions of the three allopatric lineages of *S. curicica*, reinforcing their geographic isolation. Despite the climatic stability through time on the mountaintops, divergences among the three *S. curicica* lineages are older than the modelled climatic scenarios, but still within the Pleistocene, a period characterized by global climatic oscillations (Peçanha *et al.* 2017, Cassino *et al.* 2020, Rocha *et al.* 2020). Divergence times among *B. saxicola* lineages within the Southern Espinhaço and for *B. oxente* within the north portion of the Espinhaço, also occurred during the Pleistocene, with well-structured geographic distributions on Sky Islands (Oliveira *et al.* 2021, Oswald *et al.*
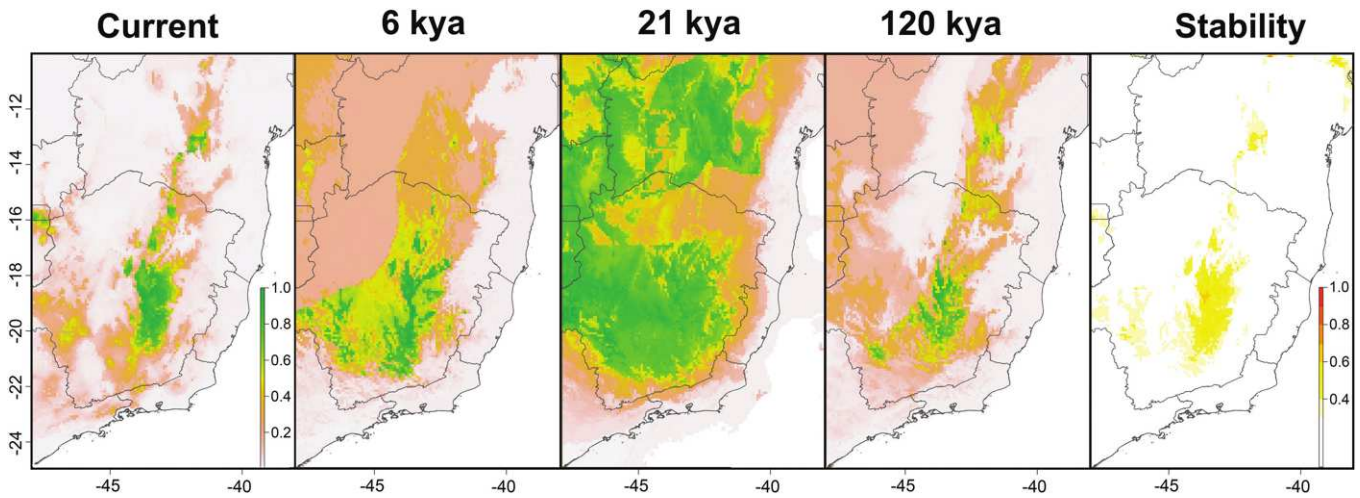
Figure 5. ENMs for *S. curicica*. From left to right, the ENM under current climate conditions, Mid-Holocene climate conditions (~6 kya), Last Glacial Maximum (LGM) climate conditions (~21 kya), Last Interglacial (LIG, ~120 kya), and regions of climate suitability through time based on all four projections.

2022). Persistence and allopatric divergence of *S. curicica* on the Sky Islands of the Espinhaço throughout the Pleistocene are consistent with results for many other amphibians in different Sky Island systems (e.g. Shepard and Burbrink 2008, Salerno *et al.* 2012, Magalhães *et al.* 2021, Ortiz *et al.* 2022). Our results provide additional support for the importance of Pleistocene climatic oscillations in promoting lineage divergence and speciation in montane anurans.

The major portions of the Espinhaço share similar geomorphological features with many mountaintops and intervening valleys within the major portions. Even these smaller valleys, which are not as low in elevation or as wide as the valleys between the major portions, can act as barriers to gene flow and promote diversification. For example, the paratelmatobiin frog, *Rupirana cardosoi*, occurs only in the northern portion of the Espinhaço (Chapada Diamantina), but two populations occur within this portion, which were recently shown to be two allopatric lineages (Santos *et al.* 2020). Many other anurans, and perhaps other dispersal-limited organisms, will probably share similar patterns of population genetic structure. The same microregional scenario could occur with other frog genera such as dwarf odontophrynids of the genus *Proceratophrys* (Teixeira Junior *et al.* 2012), the direct-developing strabomantid *Pristimantis* (Trevisan *et al.* 2020), and other treefrogs of the genus *Bokermannohyla* (Oliveira *et al.* 2021). Climatic heterogeneity in Sky Island landscapes can result in both broad- and fine-scale patterns of genetic differentiation and thus, the ecology of each species must be considered in order to understand how climatic variation affects different species (Shepard and Burbrink 2008, Gehara *et al.* 2017).

Few anuran species (or species complex) endemic to the Espinhaço are well distributed throughout the range, occurring in both its northern and southern portions. Although *Pleurodema alium* (see Maciel and Nunes 2010: fig. 4) and *Leptodactylus avivoca* (see Carvalho *et al.* 2020: fig. 1) occur in the south portion of the Espinhaço and in the Espinhaço of the Bahia State, neither of these species reach the Chapada Diamantina in fact, as they occur in an extension of the southern Espinhaço throughout Bahia. To date, *S. curicica* (Leite *et al.* 2008, present

work) and the *Odontophrynus juquinha* complex (Rocha *et al.* 2017, Moroti *et al.* 2022) are the only anurans with this distribution, occurring from southernmost Espinhaço to southern Chapada Diamantina, and revealed a similar allopatric scenario of lineage diversification. A recent evaluation of *O. juquinha* even suggested that populations from north Espinhaço (Chapada Diamantina) are a putative new species (Moroti *et al.* 2022).

Here we showed *S. curicica* is composed of three genetically and geographically distinct lineages across the Espinhaço. Following these results, we advocate for an integrative taxonomic approach including a thorough study of the acoustics, and adult and larval morphology to determine if these lineages should be considered distinct species (Padial *et al.* 2010). Until this is determined, we suggest the North and South 1 Lineages warrant special attention for conservation purposes because they occur in a small area, restricted to a few Sky Islands above 1000 m a.s.l.

SUPPLEMENTARY DATA

Supplementary data is available at *Biological Journal of the Linnean Society* online.

Table S1. Collecting localities, GenBank accession numbers, corresponding lineage for each individual sample sequenced, and voucher accession information for all samples included in the molecular analyses.

Figure S1. Plot of the number of populations simulated from the posterior distribution obtained with GENELAND for *Scinax curicica*.

ACKNOWLEDGEMENTS

DATA AVAILABILITY

The data and script supporting this study are available at: https://github.com/Rhinella85/Scinax-curicica-phylogeography
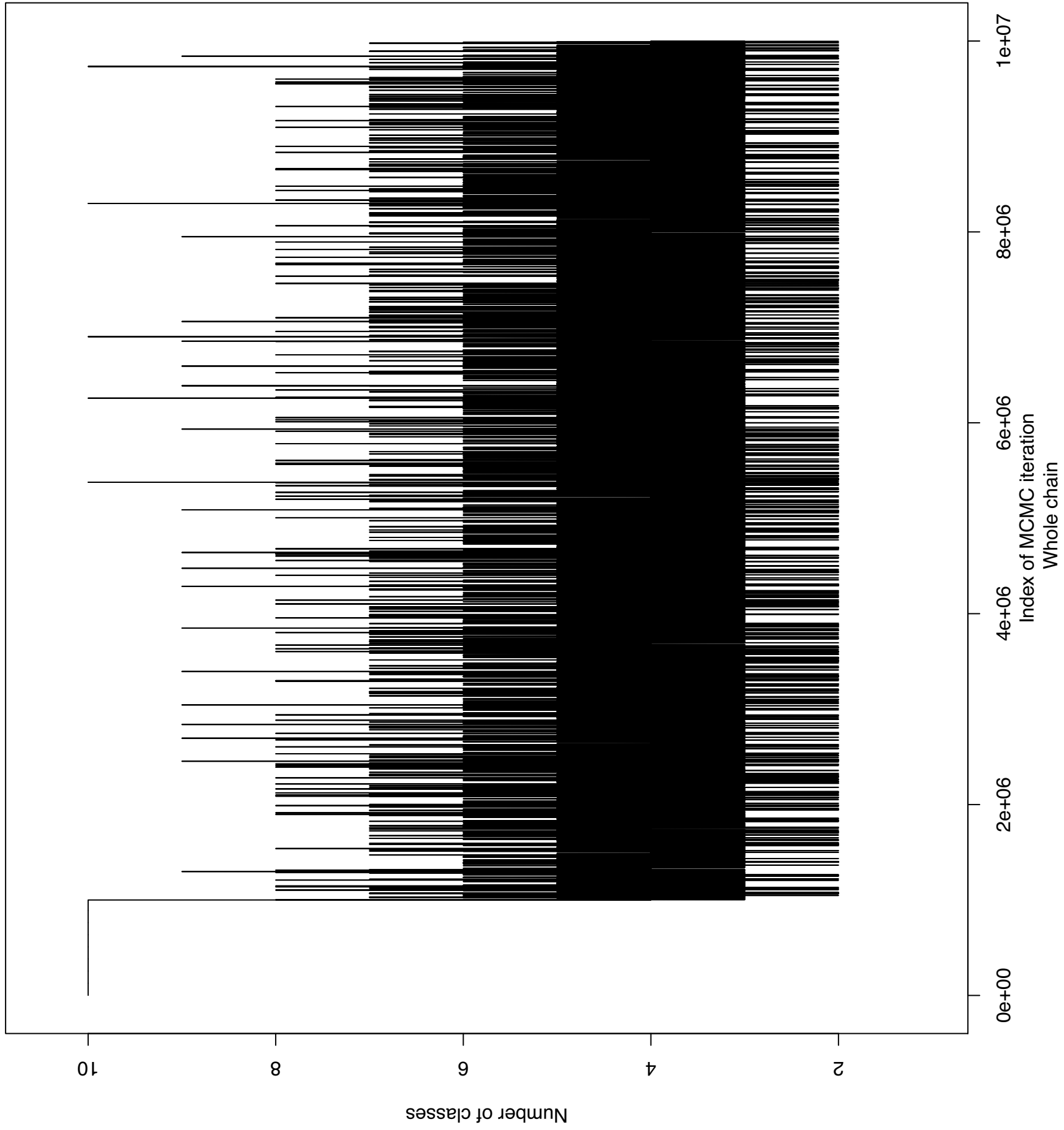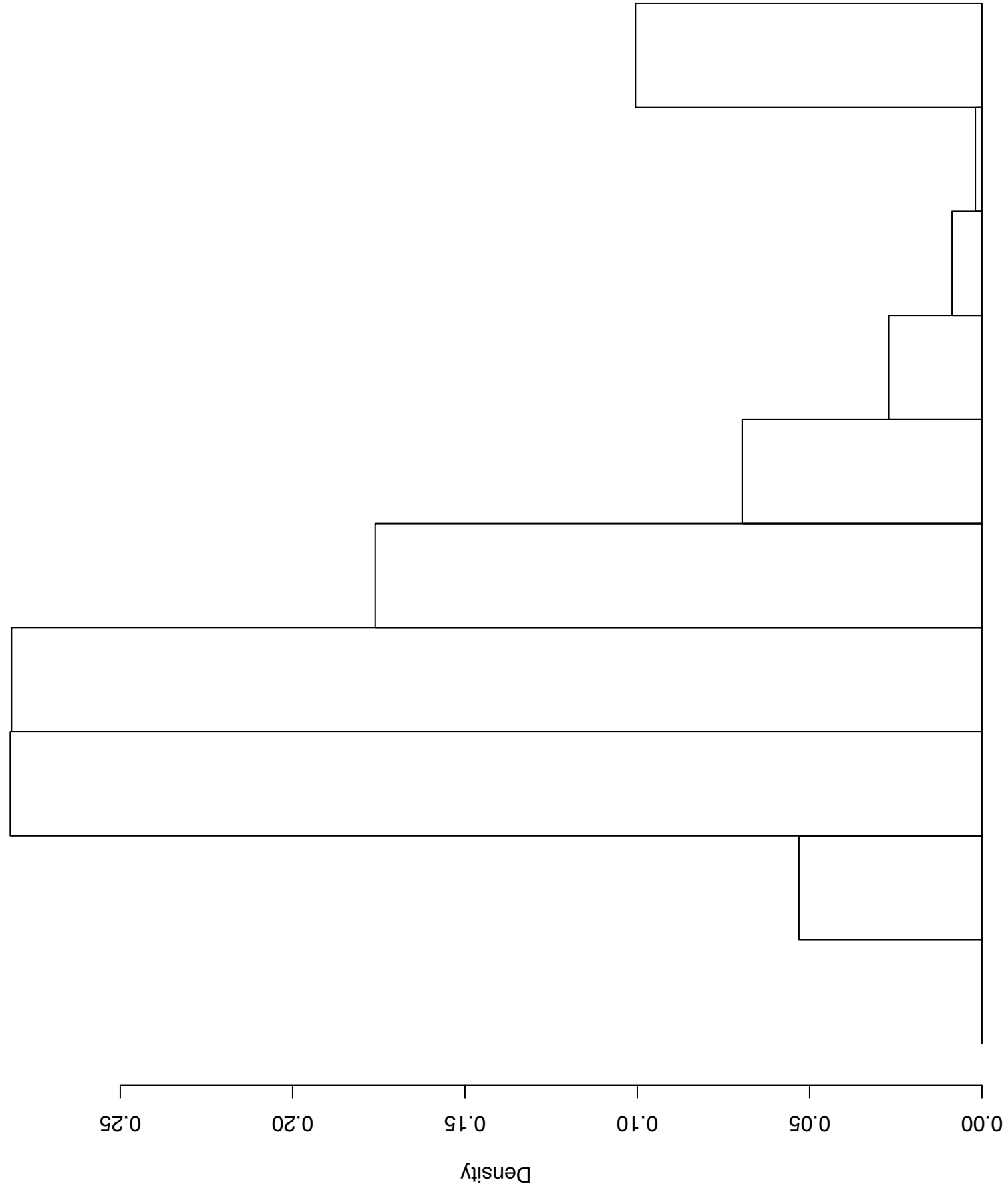
REFERENCES

Aiello-Lammens ME, Boria RA, Radosavljevic A *et al.* spThin: an R package for spatial thinning of species occurrence records for use in ecological niche models. *Ecography* 2015;**38**:541–5. https://doi.org/10.1111/ecog.01132

Bandelt HJ, Forster P, Röhl A. Median-joining networks for inferring intraspecific phylogenies. *Molecular Biology and Evolution* 1999;**16**:37–48. https://doi.org/10.1093/oxfordjournals.molbev.a026036

Barres L, Batalha-Filho H, Schnadelbach AS *et al.* Pleistocene climatic changes drove dispersal and isolation of *Richterago discoidea* (Asteraceae), an endemic plant of campos rupestres in the central and eastern Brazilian Sky Islands. *Botanical Journal of the Linnean Society* 2019;**189**:132–52. https://doi.org/10.1093/botlinnean/boy080

Beever EA, Ray C, Wilkening JL *et al.* Contemporary climate change alters the pace and drivers of extinction. *Global Change Biology* 2011;**17**:2054–70. https://doi.org/10.1111/j.1365-2486.2010.02389.x

Blair C, Bryson RW. Cryptic diversity and discordance in single-locus species delimitation methods within horned lizards (Phrynosomatidae: *Phrynosoma*). *Molecular Ecology Resources* 2017;**17**:1168–82.

Bonatelli IAS, Gehara M, Carstens BC *et al.* Comparative and predictive phylogeography in the South American diagonal of open formations: Unraveling the biological and environmental influences on multitaxon demography. *Molecular Ecology* 2021;**31**:331–42. https://doi.org/10.1111/mec.16210

Booth TH, Nix HA, Busby JR *et al.* BIOCLIM: the first species distribution modelling package, its early applications and relevance to most current MAXENT studies. *Diversity and Distributions* 2014;**20**:1–9. https://doi.org/10.1111/ddi.12144

Bossuyt F, Milinkovitch MC. Convergent adaptive radiations in Madagascan and Asian ranid frogs reveal covariation between larval and adult traits. *Proceedings of the National Academy of Sciences of the United States of America* 2000;**97**:6585–90. https://doi.org/10.1073/pnas.97.12.6585

Bouckaert R, Vaughan TG, Barido-Sottani J *et al.* BEAST 2.5: An advanced software platform for Bayesian evolutionary analysis. *PLoS Computational Biology* 2019;**15**:e1006650. https://doi.org/10.1371/journal.pcbi.1006650

Breiman L. *Classification and Regression Trees*. New York: CRC Press, 1984.

Breiman L. Random forests. *Machine Learning* 2001;**45**:5–32. https://doi.org/10.1023/A:1010933404324

Carvalho T, Sager K, Magalhães F *et al.* Systematics and cryptic diversification of *Leptodactylus* frogs in the Brazilian campo rupestre. *Zoologica Scripta* 2020;**49**:185–97. https://doi.org/10.1111/zsc.12470

Cassino RF, Ledru MP, Almeida Santos R *et al.* Vegetation and fire variability in the central Cerrados (Brazil) during the Pleistocene-Holocene transition was influenced by oscillations in the SASM boundary belt. *Quaternary Science Reviews* 2020;**232**:106209. https://doi.org/10.1016/j.quascirev.2020.106209

Collevatti RG, Terribile LC, Lima-Ribeiro MS *et al.* A coupled phylogeographical and species distribution modelling approach recovers the demographic history of a Neotropical seasonally dry forest tree species. *Molecular Ecology* 2012;**21**:5845–63. https://doi.org/10.1111/mec.12071

Costa HC, Santana DJ, Leal F *et al.* A new species of *Helicops* (Serpentes: Dipsadidae: Hydropsini) from southeastern Brazil. *Herpetologica* 2016;**72**:157–66. https://doi.org/10.1655/HERPETOLOGICA-D-15-00059

Darriba D, Taboada GL, Doallo R *et al.* JModelTest 2: More models, new heuristics and parallel computing. *Nature Methods* 2012;**9**:772. https://doi.org/10.1038/nmeth.2109

Drummond LO, Baeta D, Pires MRS. A new species of *Scinax* (Anura, Hylidae) of the *S. ruber* clade from Minas Gerais, Brazil. *Zootaxa* 2007;**1612**:45–53. https://doi.org/10.11646/zootaxa.1612.1.3

Eterovick PC. Distribution of anuran species among montane streams in southeastern Brazil. *Journal of Tropical Ecology* 2003;**19**:219–28. https://doi.org/10.1017/S0266467403003250

Ezard TH, Pearson PN, Purvis A. Algorithmic approaches to aid species' delimitation in multidimensional morphospace. *BMC Evolutionary Biology* 2010;**10**:175. https://doi.org/10.1186/1471-2148-10-175

Faivovich J, Haddad CF, Garcia PC *et al.* Systematic review of the frog family Hylidae, with special reference to Hylinae: phylogenetic analysis and taxonomic revision. *Bulletin of the American Museum of Natural History* 2005;**2005**:1–240. https://doi.org/10.1206/0003-0090(2005)294[0001:SROTFF]2.0.CO;2

Fick SE, Hijmans RJ. WorldClim 2: new 1-km spatial resolution climate surfaces for global land areas. *International Journal of Climatology* 2017;**37**:4302–15. https://doi.org/10.1002/joc.5086

Friedman JH. Multivariate adaptive regression splines. *The Annals of Statistics* 1991;**19**:1–67. https://doi.org/10.1214/aos/1176347963

Fujisawa T, Barraclough TG. Delimiting species using single-locus data and the generalized mixed yule coalescent approach: a revised method and evaluation on simulated data sets. *Systematic Biology* 2013;**62**:707–24. https://doi.org/10.1093/sysbio/syt033

García-Rodríguez A, Velasco JA, Villalobos F *et al.* Effects of evolutionary time, speciation rates and local abiotic conditions on the origin and maintenance of amphibian montane diversity. *Global Ecology and Biogeography* 2021;**30**:674–84. https://doi.org/10.1111/geb.13249

Gehara M, Crawford AJ, Orrico VG *et al.* High levels of diversity uncovered in a widespread nominal taxon: continental phylogeography of the Neotropical tree frog *Dendropsophus minutus*. *PLoS One* 2014;**9**:e103958. https://doi.org/10.1371/journal.pone.0103958

Gehara M, Garda AA, Werneck FP *et al.* Estimating synchronous demographic changes across populations using hABC and its application for a herpetological community from northeastern Brazil. *Molecular Ecology* 2017;**26**:4756–71.

Graham CH, Carnaval AC, Cadena CD *et al.* The origin and maintenance of montane diversity: Integrating evolutionary and ecological processes. *Ecography* 2014;**37**:711–9. https://doi.org/10.1111/ecog.00578

Guedes TB, Azevedo JAR, Bacon CD *et al.* Diversity, endemism, and evolutionary history of montane biotas outside the Andean region. In: Rull V, Carnaval A (eds.), *Neotropical Diversification: Patterns and Processes*. Berlin: Springer, 2020, 299–328. https://doi.org/10.1007/978-3-030-31167-4_13

Guillot G, Mortier F, Estoup A. GENELAND: a computer package for landscape genetics. *Molecular Ecology Notes* 2005;**5**:712–5. https://doi.org/10.1111/j.1471-8286.2005.01031.x

Haffer J, Prance GT. Impulsos climáticos da evolução na Amazônia durante o Cenozóico: sobre a teoria dos Refúgios da diferenciação biótica. *Estudos avançados* 2002;**16**:175–206.

Hastie T, Tibshirani R. Exploring the nature of covariate effects in the proportional hazards model. *Biometrics* 1990;**46**:1005–16. https://doi.org/10.2307/2532444

Hastie T, Tibshirani R, Buja A. Flexible discriminant analysis by optimal scoring. *Journal of the American Statistical Association* 1994;**89**:1255–70.

Irwin DL, Mitchelson KR, Findlay I. PCR product cleanup methods for capillary electrophoresis. *Biotechniques* 2003;**34**:932–4, 936.

Juncá FA, Napoli MF, Nunes I *et al.* A new species of the *Scinax ruber* clade (Anura, Hylidae) from the Espinhaço Range, northeastern Brazil. *Herpetologica* 2015;**71**:299–309. https://doi.org/10.1655/HERPETOLOGICA-D-14-00032

Kapli P, Lutteropp S, Zhang J *et al.* Multi-rate Poisson tree processes for single-locus species delimitation under maximum likelihood and Markov chain Monte Carlo. *Bioinformatics* 2017;**33**:1630–8.

Leigh JW, Bryant D. POPART: full-feature software for haplotype network construction. *Methods in Ecology and Evolution* 2015;**6**:1110–6. https://doi.org/10.1111/2041-210X.12410

Leite FSF, Pezzuti TL, Viana PL. Amphibia, *Bokermannohyla nanuzae, Scinax curicica, Leptodactylus camaquara, Physalaemus evangelistai* and *Proceratophrys cururu*: Distribution extensions. *Check List* 2006;**2**:5. https://doi.org/10.15560/2.1.5

Leite FSF, Eterovick PC, Juncá FA. Status do conhecimento, endemismo e conservação de anfíbios anuros da Cadeia do Espinhaço, Brasil. *Megadiversidade* 2008;**4**:158–76.

Maciel DB, Nunes I. A new species of four-eyed frog genus *Pleurodema* Tschudi, 1838 (Anura: Leiuperidae) from the rock meadows of Espinhaço range, Brazil. *Zootaxa* 2010;**2640**:53–61. https://doi.org/10.11646/zootaxa.2640.1.4

Magalhães RF, Lemes P, Camargo A *et al*. Evolutionarily significant units of the critically endangered leaf frog *Pithecopus ayeaye* (Anura, Phyllomedusidae) are not effectively preserved by the Brazilian protected areas network. *Ecology and Evolution* 2017;**7**:8812–28. https://doi.org/10.1002/ece3.3261

Magalhães RF, Lemes P, Santos MTT *et al*. Evidence of introgression in endemic frogs from the campo rupestre contradicts the reduced hybridization hypothesis. *Biological Journal of the Linnean Society* 2021;**133**:561–76. https://doi.org/10.1093/biolinnean/blaa142

Mângia S, Oliveira EF, Santana DJ *et al*. Revising the taxonomy of *Proceratophrys* Miranda-Ribeiro, 1920 (Anura: Odontophrynidae) from the Brazilian semiarid Caatinga: Morphology, calls and molecules support a single widespread species. *Journal of Zoological Systematics and Evolutionary Research* 2020;**58**:1151–72. https://doi.org/10.1111/jzs.12365

McCormack JE, Heled J, Delaney KS *et al*. Calibrating divergence times on species trees versus gene trees: Implications for speciation history of *Aphelocoma* jays. *Evolution* 2011;**65**:184–202. https://doi.org/10.1111/j.1558-5646.2010.01097.x

McCullagh P, Nelder JA. *Generalized Linear Models, 2nd edn*. New York: Chapman and Hall, 1989.

Miola DT, Ramos VD, Silveira FA. A brief history of research in campo rupestre: Identifying research priorities and revisiting the geographical distribution of an ancient, widespread Neotropical biome. *Biological Journal of the Linnean Society* 2021;**133**:464–80. https://doi.org/10.1093/biolinnean/blaa175

Moroti MT, Pedrozo M, Severgnini MR *et al*. A new species of *Odontophrynus* (Anura, Odontophrynidae) from the southern portion of the Mantiqueira mountains. *European Journal of Taxonomy* 2022;**847**:160–93. https://doi.org/10.5852/ejt.2022.847.1991

Naimi B. *Package 'usdm'. Uncertainty Analysis for Species Distribution Models. R-Cran, 18*, 2017. https://cran.r-project.org/web/packages/usdm/usdm.pdf

Nascimento AC, Chaves AV, Leite FSF *et al*. Past vicariance promoting deep genetic divergence in an endemic frog species of the Espinhaço Range in Brazil: The historical biogeography of *Bokermannohyla saxicola* (Hylidae). *PLoS One* 2018;**13**:e0206732. https://doi.org/10.1371/journal.pone.0206732

Oliveira FFR, Gehara M, Solé M *et al*. Quaternary climatic fluctuations influence the demographic history of two species of sky-island endemic amphibians in the Neotropics. *Molecular Phylogenetics and Evolution* 2021;**160**:107113. https://doi.org/10.1016/j.ympev.2021.107113

Ortiz DA, Hoskin CJ, Werneck FP *et al*. Historical biogeography highlights the role of Miocene landscape changes on the diversification of a clade of Amazonian tree frogs. *Organisms Diversity & Evolution* 2022;**23**:395–414. https://doi.org/10.1007/s13127-022-00588-2

Oswald CB, Lemes P, Thomé MTC *et al*. Colonization rather than fragmentation explains the geographical distribution and diversification of treefrogs endemic to Brazilian shield Sky Islands. *Journal of Biogeography* 2022;**49**:682–98. https://doi.org/10.1111/jbi.14320

Padial JM, Miralles A, De la Riva I *et al*. The integrative future of taxonomy. *Frontiers in Zoology* 2010;**7**:16–4. https://doi.org/10.1186/1742-9994-7-16

Palumbi SR, Martin A, Romano S *et al*. *The Simple Fool's Guide to PCR, Version 2.0*. Honolulu: University of Hawaii, 1991, 45. https://doi.org/10.1186/s13620-015-0060-3

Pan T, Wang H, Orozcoterwengel P *et al*. Long-term Sky Islands generate highly divergent lineages of a narrowly distributed stream salamander (*Pachyhynobius shangchengensis*) in mid-latitude mountains of East Asia. *BMC Evolutionary Biology* 2019;**19**:1–15. https://doi.org/10.1186/s12862-018-1333-8

Paradis E, Claude J, Strimmer K. APE: Analyses of phylogenetics and evolution in R language. *Bioinformatics* 2004;**20**:289–90. https://doi.org/10.1093/bioinformatics/btg412

Peçanha WT, Althoff SL, Galiano D *et al*. Pleistocene climatic oscillations in Neotropical open areas: refuge isolation in the rodent *Oxymycterus nasutus* endemic to grasslands. *PLoS One* 2017;**12**:e0187329. https://doi.org/10.1371/journal.pone.0187329

Phillips SJ, Anderson RP, Schapire RE. Maximum entropy modeling of species geographic distributions. *Ecological Modelling* 2006;**190**:231–59. https://doi.org/10.1016/j.ecolmodel.2005.03.026

Pie MR, Faircloth BC, Ribeiro LF *et al*. Phylogenomics of montane frogs of the Brazilian Atlantic Forest is consistent with isolation in Sky Islands followed by climatic stability. *Biological Journal of the Linnean Society* 2018;**125**:72–82. https://doi.org/10.1101/226159

Pugliese A, Pombal JP Jr, Sazima I. A new species of *Scinax* (Anura: Hylidae) from rocky montane fields of the Serra do Cipó, southeastern Brazil. *Zootaxa* 2004;**688**:1–15. https://doi.org/10.11646/zootaxa.688.1.1

R Core Team. *R: A Language and Environment for Statistical Computing*. Vienna: R Foundation for Statistical Computing, 2015. https://www.R-project.org/

R Core Team. *R: A Language and Environment for Statistical Computing*. Vienna: R Foundation for Statistical Computing, 2021. https://www.R-project.org/

R Core Team. *R: A Language and Environment for Statistical Computing*. Vienna: R Foundation for Statistical Computing, 2023. https://www.R-project.org/

Rahbek C, Borregaard MK, Colwell RK *et al*. Humboldt's enigma: what causes global patterns of mountain biodiversity? *Science* 2019;**365**:1108–13. https://doi.org/10.1126/science.aax0149

Rambaut A, Drummond AJ, Xie D *et al*. Posterior summarization in Bayesian phylogenetics using Tracer 1.7. *Systematic Biology* 2018;**67**:901–4. https://doi.org/10.1093/sysbio/syy032

Ridgeway G. The state of boosting. *Computing Science and Statistics* 1999;**31**:172–81.

Rocha PC, Sena LMF, Pezzuti TL *et al*. A new diploid species belonging to the *Odontophrynus americanus* species group (Anura: Odontophrynidae) from the Espinhaço range, Brazil. *Zootaxa* 2017;**4329**:327–50. https://doi.org/10.11646/zootaxa.4329.4.2

Rocha AV, Cabanne GS, Aleixo A *et al*. Pleistocene climatic oscillations associated with landscape heterogeneity of the South American dry diagonal explains the phylogeographic structure of the narrow-billed woodcreeper (*Lepidocolaptes angustirostris*, Dendrocolaptidae). *Journal of Avian Biology* 2020;**51**:1–13. https://doi.org/10.1111/jav.02537

Rozas J, Ferrer-Mata A, Sanchez-Del Barrio JC *et al*. DnaSP 6: DNA sequence polymorphism analysis of large data sets. *Molecular Biology and Evolution* 2017;**34**:3299–302. https://doi.org/10.1093/molbev/msx248

Salerno PE, Ron SR, Senaris JC *et al*. Ancient tepui summits harbor young rather than old lineages of endemic frogs. *Evolution* 2012;**66**:3000–13. https://doi.org/10.1111/j.1558-5646.2012.01666.x

Santos MTT, Magalhães RF, Lyra ML *et al*. Multilocus phylogeny of Paratelmatobiinae (Anura: Leptodactylidae) reveals strong spatial structure and previously unknown diversity in the Atlantic Forest hotspot. *Molecular Phylogenetics and Evolution* 2020;**148**:106819. https://doi.org/10.1016/j.ympev.2020.106819

Schaefer CE, Corrêa GR, Candido HG *et al*. The physical environment of rupestrian grasslands (Campos Rupestres) in Brazil: geological, geomorphological and pedological characteristics, and interplays. In: Fernandes GW (ed.), *Ecology and Conservation of Mountaintop Grasslands in Brazil. Cham: Springer*, 2016, 15–53. https://doi.org/10.1007/978-3-319-29808-5_2

Sekar S, Karanth P. Flying between Sky Islands: the effect of naturally fragmented habitat on butterfly population structure. *PLoS One* 2013;**8**:e71573. https://doi.org/10.1371/journal.pone.0071573

Shepard DB, Burbrink FT. Lineage diversification and historical demography of a sky island salamander, *Plethodon ouachitae*, from the Interior Highlands. *Molecular Ecology* 2008;**17**:5315–35. https://doi.org/10.1111/j.1365-294X.2008.03998.x

Shepard DB, Burbrink FT. Phylogeographic and demographic effects of Pleistocene climatic fluctuations in a montane salamander, *Plethodon fourchensis*. *Molecular Ecology* 2009;**18**:2243–62. https://doi.org/10.1111/j.1365-294x.2009.04164.x

Silveira FA, Negreiros D, Barbosa NP *et al.* Ecology and evolution of plant diversity in the endangered campo rupestre: a neglected conservation priority. *Plant and Soil* 2016;**403**:129–52. https://doi.org/10.1007/s11104-015-2637-8

Sinervo B, Mendez-de-la-Cruz F, Miles DB *et al.* Erosion of lizard diversity by climate change and altered thermal niches. *Science* 2010;**328**:894–9. https://doi.org/10.1126/science.1184695

Teixeira Junior M, Amaro RC, Recoder RS *et al*. A new dwarf species of *Proceratophrys* Miranda-Ribeiro, 1920 (Anura, Cycloramphidae) from the highlands of Chapada Diamantina, Bahia, Brazil. *Zootaxa* 2012;**3551**:25–42. https://doi.org/10.11646/zootaxa.3551.1.2

Thuiller W, Georges D, Engler R *et al. Package 'biomod2'*, 2016. https://cran.r-project.org/web/packages/biomod2/index.html

Trevisan CC, Batalha-Filho H, Garda AA *et al*. Cryptic diversity and ancient diversification in the northern Atlantic Forest *Pristimantis* (Amphibia, Anura, Craugastoridae). *Molecular Phylogenetics and Evolution* 2020;**148**:106811. https://doi.org/10.1016/j.ympev.2020.106811

Number of clusters along the chain after burnin

Density

Nb. of clusters along the chain
(after a burnin of 0x1000i t.)

Number of classes

Index of MCMC iteration
Whole chain

1 **Table S1.** Collecting localities, GenBank accession numbers sequence data, the corresponding lineage for each individual sample sequenced, and the voucher

2 accession information for all samples included in molecular analyses. PARNA (Parque Nacional)

3 * *S. curicica* type locality.

Municipality	Locality	Brazilian State	Latitude	Longitude	Genbank Accession		Lineage	Voucher specimen
					16s	Rhodopsin		
Mucugê	Serra do Sincorá	BA	-13.00883	-41.37118	MZ606705	-	N	UFMG4266
Mucugê	Serra do Sincorá	BA	-13.00883	-41.37118	MZ606706	MZ615207	N	UFMG4267
Mucugê	Serra do Sincorá	BA	-13.00883	-41.37118	MZ606707	MZ615208	N	UFMG4268
Mucugê	Serra do Sincorá	BA	-13.00883	-41.37118	MZ606708	MZ615209	N	UFMG4269
Mucugê	Serra do Sincorá	BA	-13.00883	-41.37118	MZ606709	-	N	UFMG4270
Mucugê	Serra do Sincorá	BA	-13.00883	-41.37118	MZ606710	-	N	UFMG4271
Palmeiras	Serra do Sincorá	BA	-12.56067	-41.56124	MZ606691	MZ615211	N	UFMG4540
Palmeiras	Serra do Sincorá	BA	-12.56067	-41.56124	-	MZ615212	N	UFMG4542
Palmeiras	Serra do Sincorá	BA	-12.56067	-41.56124	MZ606711	MZ615213	N	UFMG4543
Palmeiras	Serra do Sincorá	BA	-12.56067	-41.56124	MZ606712	MZ615214	N	UFMG4544
Palmeiras	Serra do Sincorá	BA	-12.56067	-41.56124	-	MZ615215	N	UFMG4548
Palmeiras	Serra do Sincorá	BA	-12.56067	-41.56124	MZ606713	MZ615216	N	UFMG4570
Palmeiras	Serra do Sincorá	BA	-12.56067	-41.56124	MZ606714	MZ615217	N	UFMG4574

Municipality	Locality	State	Latitude	Longitude			N	
Rio de Contas	Serra das Almas	BA	-13.58584	-41.81362	-	MZ615210	N	UFMG4467
Barão de Cocais	Serra do Garimpo	MG	-19.94167	-43.48257	MZ606703	MZ615205	S2	UFMG14934
Catas Altas	Serra do Caraça	MG	-20.07389	-43.40652	-	MZ615206	S2	UFMG1771
Congonhas do Norte	-	MG	-18.81078	-43.67853	MZ606704	-	S2	UFMG4037
Congonhas do Norte	-	MG	-18.81078	-43.67853	-	MZ615224	S2	UFMG6676
Congonhas do Norte	-	MG	-18.81078	-43.67853	-	MZ615225	S2	UFMG6677
Congonhas do Norte	-	MG	-18.81078	-43.67853	MZ606718	MZ615226	S2	UFMG6678
Diamantina	Serra D'anta	MG	-18.24627	-43.6041		MZ615192	S2	UFMG10723
Diamantina	PARNA Sempre Vivas	MG	-18.24627	-43.6041	-	MZ615204	S2	UFMG12166
Diamantina	PARNA Sempre Vivas	MG	-18.24627	-43.6041	MZ606700	-	S2	UFMG12167
Itacambira	Serra de Itacambira	MG	-17.06295	-43.30734	MZ606699	-	S1	UFMG9341
Itacambira	Serra de Itacambira	MG	-17.06295	-43.30734	MZ606694	MZ615198	S1	UFMG11253
Itacambira	Serra de Itacambira	MG	-17.06295	-43.30734	MZ606695		S1	UFMG11255
Itacambira	Serra de Itacambira	MG	-17.06295	-43.30734	MZ606696	MZ615199	S1	UFMG11269
Itacambira	Serra de Itacambira	MG	-17.06295	-43.30734	MZ606697	MZ615200	S1	UFMG11351
Itacambira	Serra de Itacambira	MG	-17.06295	-43.30734	-	MZ615201	S1	UFMG11353
Itacambira	Serra de Itacambira	MG	-17.06295	-43.30734	MZ606698	MZ615202	S1	UFMG11357
Mariana	Chapada de Canga	MG	-20.36581	-43.41463	MZ606715	MZ615218	S2	UFMG5368

Municipality	Locality	State	Latitude	Longitude			Clade	Voucher
Mariana	Chapada de Canga	MG	-20.36581	-43.41463	MZ606716	MZ615219	S2	UFMG5373
Mariana	Chapada de Canga	MG	-20.36581	-43.41463	-	MZ615220	S2	UFMG5375
Mariana	Chapada de Canga	MG	-20.36581	-43.41463	-	MZ615203	S2	UFMG11677
Rio Pardo de Minas	Serra Nova	MG	-15.61753	-42.54384	-	MZ615221	S1	UFMG6004
Rio Pardo de Minas	Serra Nova	MG	-15.61753	-42.54384	-	MZ615222	S1	UFMG6037
Rio Pardo de Minas	Serra Nova	MG	-15.61753	-42.54384	MZ606717	-	S1	UFMG6038
Rio Pardo de Minas	Serra Nova	MG	-15.61753	-42.54384	-	MZ615223	S1	UFMG6042
Rio Pardo de Minas	Serra Nova	MG	-15.61753	-42.54384	-	MZ615227	S1	UFMG6854
Rio Vermelho	Serra do Ambrósio	MG	-18.24718	-43.05826	MZ606688	MZ615193	S2	UFMG10845
Rio Vermelho	Serra do Ambrósio	MG	-18.24718	-43.05826	MZ606690	MZ615194	S2	UFMG10847
Rio Vermelho	Serra do Ambrósio	MG	-18.24718	-43.05826	-	MZ615195	S2	UFMG10849
Rio Vermelho	Serra do Ambrósio	MG	-18.24718	-43.05826	MZ606692		S2	UFMG10850
Rio Vermelho	Serra do Ambrósio	MG	-18.24718	-43.05826	-	MZ615196	S2	UFMG10851
Rio Vermelho	Serra do Ambrósio	MG	-18.24718	-43.05826	-	MZ615197	S2	UFMG10852
Rio Vermelho	Serra do Ambrósio	MG	-18.24718	-43.05826	MZ606693		S2	UFMG10853
Rio Vermelho	Serra do Ambrósio	MG	-18.24718	-43.05826	MZ606689		S2	UFMG10855
Santana do Riacho*	Serra do Cipó	MG	-19.1694	-43.7148	KY002954	-	S2	MCNAM 19675
Santana do Riacho*	Serra do Cipó	MG	-19.1694	-43.7148	KY007114	-	S2	MCNAM 14162

| Santo Antônio do Itambé | Pico do Itambé | MG | -18.47091 | -43.27184 | MZ606702 | - | S2 | UFMG14756 |
| Santo Antônio do Itambé | Pico do Itambé | MG | -18.47091 | -43.27184 | MZ606701 | - | S2 | UFMG14791 |

4

5